Giant Axial Electrostrictive Deformation in Carbon Nanotubes

Wanlin Guo* and Yufeng Guo

Institute of Nano Science, Nanjing University of Aeronautics and Astronautics, Nanjing, 210016, China

(Received 16 April 2003; published 9 September 2003)

An exceptionally large axial electrostrictive deformation is demonstrated in single walled carbon nanotubes using Hartree-Fock and density functional quantum mechanics simulations. Armchair and zigzag open-ended tubes and capped tubes are studied and in all of them the external electric field induced axial strains can be greater than 10% for a field strength within 1 V/Å. The corresponding volumetric and gravimetric work capacities are predicted to be three and six orders higher than those of the best known ferroelectric, electrostrictive, magnetostrictive materials and elastomers, respectively.

DOI: 10.1103/PhysRevLett.91.115501 PACS numbers: 61.46.+w, 77.65.–j

The mechanisms for converting electrical energy into mechanical energy are essential for the design of diverse nanoscale devices. Materials having piezoelectric, electrostrictive, and electrochemical properties play important roles in the conversion between electrical and mechanical energy. Piezoelectric materials, especially piezoceramics, are widely used as sensors and actuators, but their deformation is too small, about 0.1% strain with low fracture toughness. Electroactive polymers (EAPs) exhibit strain levels far above those of traditional piezoelectric materials but have a low dielectric constant [1]. An all-organic EAP composite has been designed to provide a high dielectric constant and raise the strain up to 2% with an elastic modulus around 1 GPa [2]. An exceptionally high electrostrictive response ($\sim 4\%$) was observed in an electron irradiated copolymer [3]. To achieve higher electrostrictive strain, microfabricated conjugated polymer actuators and electrostatic compressible structures from films of dielectric elastomers coated with compliant electrode materials have been designed [4,5]. However, the work densities of these materials or systems are low. To achieve a high actuation strain and high work density simultaneously is an attractive but challenging goal, especially in nanoscale devices.

Carbon nanotubes (CNTs) are up to 100 times stronger than steel, lightweight, and able to withstand repeated loading. They have, in air and at room temperature, a Young's modulus of 0.64 TPa or higher, and an elongation at break of 30% [6]. The CNTs have an exceptional conductivity and high sensitivity to applied fields as well [7–12]. A sheet of single walled CNTs (SWNTs) can expand the tubes along its own length for about 1% and function as artificial muscles when charged in an electrolyte [8]. The flow of a polar liquid over a SWNT bundle can generate voltage in the tubes [9]. The electrical resistance of a semiconducting SWNT was found to change dramatically upon exposure to some gaseous molecules [10]. CNTs can be reoriented [11], broken, and stretched straightly [12] under external applied electric fields. All the facts show that CNTs are potential novel intelligent nanomaterials sensitive to external environments and electric fields. But until the present, only 1% actuation strain is reported in CNT sheets caused by electrochemical dopant intercalation [8]. In this Letter, we demonstrate extremely large axial electrostrictive deformation, or the deformation induced by applied electrostatic field, larger than 12% in CNTs by detailed Hartree-Fock (HF) *ab initio* quantum mechanics and density function theory (DFT) simulations. The physical mechanism of the large electrostrictive deformation of CNTs is explained by delicate shifting in electronic structures of the tube shell.

In this study, we considered single-wall (3, 3) and (5, 0) open-ended CNTs and (5, 5) nanotube with a capped edge. Two lengths of the armchair (3, 3) nanotubes are modeled, one with five layers of carbon rings (42 carbon atoms) and the other with 11 layers of carbon rings (66 carbon atoms), to show the length effect. The zigzag (5, 0) nanotube is similarly constructed with four layers of carbon rings (40 carbon atoms). The dangling bonds at the open ends of the (3, 3) and (5, 0) nanotubes are free from any attachment. The armchair (5, 5) nanotube is modeled by five layers of carbon rings (50 carbon atoms) along the tube axial where one end is capped with C_{30} and dangling bonds at the other end are saturated by hydrogen atoms in order to emulate an infinite tube. When the external field is considered, a uniform electric field is applied parallel to the tube axis. The total energy minimization method with quantum mechanical calculations is implemented to investigate the equilibrium structures of SWNTs under external electric fields.

The total energy calculations and corresponding structure optimizations for the nanotubes with and without external applied electric fields are performed by using both the Hartree-Fock and density functional formalism as described at the end of this Letter. However, all the electronic structures are obtained by the density functional technique on the basis of the optimized geometry.

The initial length of the (3, 3)/42 (42 carbon atoms) tube in the released state without applied field is 0.712 nm and the length of the (3, 3)/66 tube is 1.204 nm by both of the techniques. Some typical curves of the axial deformation ratio of the nanotube vs the strength of the external electric field are presented in Fig. 1. The electrostrictive deformation of the (3, 3)/42 tube reaches 2% at electric

field strength of 0.06 V/Å, 4% at 0.17 V/Å, 11% at 0.36 V/Å, and 13% at 0.41 V/Å. The discrepancy between the HF and DFT calculations of axial deformation is less than 3.5%. This good coincidence confirms the giant axial electrostrictive deformation in the SWNT.

The electrostrictive deformation ratio in a semimetallic (5, 0) tube, whose initial length is 0.697 nm, is slightly lower than that in a (3, 3) tube having similar size, but the ratio is in the same level. The size effect can also be seen from the figure. When the initial tube length increases from 0.712 nm of the (3, 3)/42 by 69% to 1.204 nm of the (3, 3)/66, the electrostrictive deformation remains the same when the electric field strength is lower than 0.2 V/Å, and gets smaller at higher electric field strength, but still can reach 10% at 0.41 V/Å.

The capped (5, 5) tube with a hydrogen saturated end has a much larger diameter as well as a different geometry and end condition in comparison with the open-ended (3, 3) and (5, 0) tubes. When it is put into the electric field, giant electrostrictive deformation can be demonstrated by the DFT simulation as well. The elongation ratio can be up to 12.05% at an electric field strength of 1 V/Å.

The axial deformation of a CNT comes from two aspects of geometrical changes: the elongation of the C-C bonds and the distortion of the carbon hexagonal rings. A detailed investigation shows that with increasing electric field strength, there is no systematical change in bond angles for contribution to axial extension. The C-C bond lengths, however, are found to be sensitive to the electric field. In Fig. 2, the average elongation ratio of the C-C bonds which contributes to the axial deformation is drawn against the electric field strength. Comparing with the axial deformation ratio shows that the C-C bond elongation is the only significant contribution to the electrostrictive deformation. At an electric field strength higher than 0.2 V/Å, the DFT results of bond elongation are slightly higher than the HF results. When the (3, 3)/42 tube is unwrapped into a planar graphite sheet of the same atoms in the same orientation to the applied field, however, the HF simulated electrostrictive deformation reaches a saturation value less than 2.6% when the field strength is greater than about 0.15 V/Å. In fact, the C-C bond elongation at the edges of the sheet becomes highly localized even at 0.155 V/Å. This means that the sheet has much lower critical average strain and field strength of breakdown than the nanotube. For a planar graphite sheet from an unwrapped (5, 0)/40 zigzag tube, the localization of the C-C bond elongation at the edges of the sheet is much stronger, the electrostriction deformation of the sheet is 1.55% at a field strength of 0.155 V/Å, and unstable failure occurs at 0.361 V/Å.

The deeper reason for the electrostrictive deformation should be the change in the electric structures of CNTs. In the released state of equilibrium without external fields, the total charge distribution slightly deviates from the electric neutral state and no polarization existed in both the (3, 3) and (5, 0) tubes. When the external electric field is applied, the total charge distribution remains nearly the same as in the released state for the field strength up to 0.41 V/Å in both kinds of tubes, and no obvious total charge polarization occurs. A previous study showed that only when the strength of the applied electric field is greater than about 3 V/Å can a remarkable total charge polarization occur [13]. In contrast, the distributions of the charge density of the highest occupied molecular orbital (HOMO) and the lowest unoccupied molecular orbital (LUMO) are very sensitive to the applied electric field even for very low field strength. Figure 3 shows typical results for the distribution of charge density of

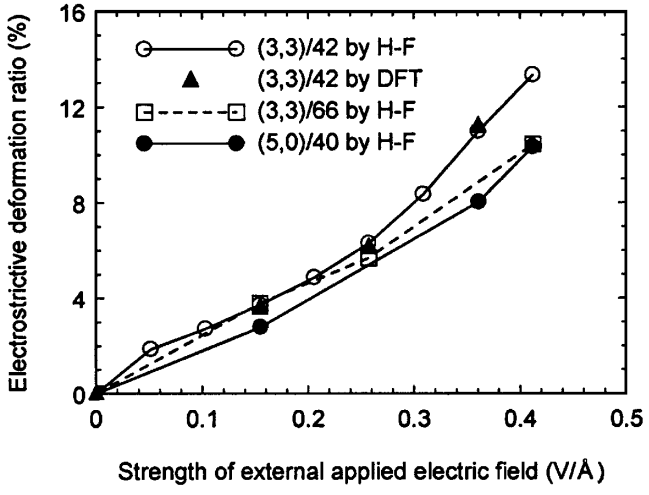

FIG. 1. Axial electrostrictive deformation ratio induced by external applied electric field in (3, 3) metallic single walled CNTs of different lengths and a (5, 0) semi-metallic tube.

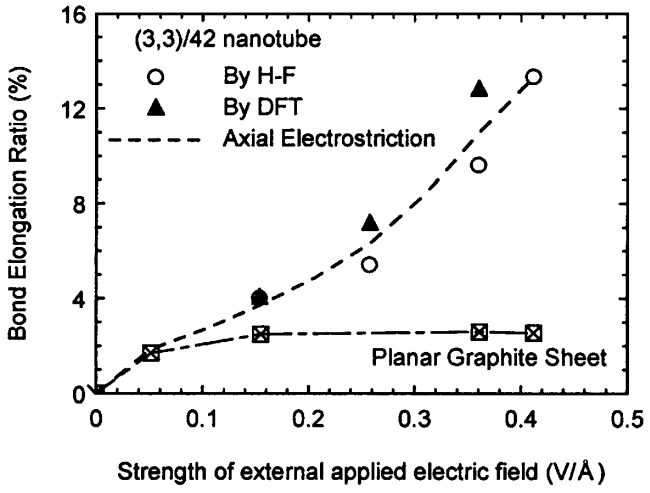

FIG. 2. Average elongation ratios of the C-C bonds having a contribution to the deformation along the direction of the external electric field for the (3, 3)/42 tube and the corresponding planar graphite sheet.

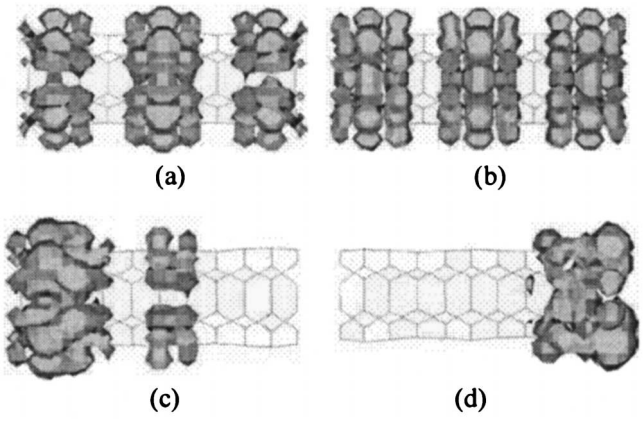

FIG. 3. The contour plots of charge density [in units of $0.0005e/(\text{a.u.})^3$] for the electron structures of the (3, 3)/66 tube predicted by the DFT technique. (a) Charge density of the HOMO with energy of −3.28 eV, and (b) charge density of the LUMO with energy of −0.61 eV in the released state. (c) Charge density of the HOMO with energy of −12.71 eV, and (d) charge density of the LUMO with energy of −10.70 eV under the electric field of 0.361 V/Å.

HOMO and LUMO in the (3, 3)/66 tube in the released state and in an applied electric field with a strength of 0.361 V/Å. An increase in the electric field strength from 0 to 0.361 V/Å causes the highest occupied level polarization. The HOMO energy changes from −3.28 to −12.712 eV, the LUMO energy changes from −0.61 to −10.703 eV, and the energy gap between them changes from 2.67 to 2.009 eV in the tube. Similar results are obtained for the shorter (3, 3)/42 tube. In this Letter, the DFT results are used for discussions of the electron structures as the DFT technique is generally recognized to provide a better prediction for electron structures, although it is much more time consuming.

In the (5, 0) tube, for the same change in electric field strength, from 0 to 0.361 V/Å, the energy of HOMO changes from −3.736 to −12.607 eV, the energy of LUMO changes from −2.688 to −11.066 eV and the energy gap changes from 1.047 to 1.541 eV. In the capped (5, 5) nanotube, the energy gap decreases from 1.34 eV at the initial state to 0.94 eV in the electrostrictive state at 1 V/Å applied field strength.

In addition to having a large axial electrostrictive deformation, the exceptional high Yang's modulus and strength of CNTs make them ultrahigh-performance actuator materials. The volumetric and gravimetric work densities per cycle for a matched mechanical load are proportional to $1/2Y\varepsilon_m^2$ and $1/2Y\varepsilon_m^2/\rho$, respectively, where ε_m is the maximum axial strain and ρ is the density (1.33 g/cm^3) of the CNTs [8]. Based on the theoretical and experimental results of $Y \sim 0.64$ TPa [6] for SWNTs and our present result of $\varepsilon_m \sim 10\%$, a volumetric work capacity is predicted to be three orders higher than has been tabulated [14] for the best known ferroelectric, electrostrictive, and magnetostrictive materials and the electrical actuators from films of dielectric elastomers [4]. The gravimetric work capacity of the present axial electrostrictive actuator is six orders higher than the tabulated materials. Even when 1% volumetric SWNTs composite is made with nonelectrostrictive matrix materials, an increasing factor about 216 in gravimetric work capacity can be expected against the tabulated materials [14].

In the above simulation, uniform external fields are applied around the CNTs and the length to diameter ratio considered in this work is small, so the field enhancement factor is near unity. In a practical setup, the external applied field may be magnified by a field enhancement factor up to the order of 10^3 near the tips of CNTs because of their large length to diameter ratio [15,16]. It can be expected that such a high field enhancement factor may remarkably reduce the required applied field strength to produce the exceptional high electrostrictive deformation ($> 10\%$). The extremely large electrostrictive deformation may be observed with the state of art techniques, such as Wang's setup [12]. As nanosystems may allow for the application of high electric or magnetic fields which can be comparable to the local atomic fields, it will be interesting to investigate whether similar exceptional phenomena exist in other nanomaterials or systems, and the size effects of such exceptional properties will be challenging topics for further physical mechanics study.

The density functional technique is within the linear combination of atomic orbitals assumption and the local density approximation. All-electron Kohn-Sham wave functions are expanded in a local atomic orbital basis. The numerical free-atom basis sets (STO-3G) selected are $2s2p$ atomic orbitals for carbon atoms, and a $3d$-type wave function on each carbon atom is used to describe the polarization. The Hartree-Fock *ab initio* technique is based on the Roothaan-Hall equations which adopt the self-consistent field approach and the Fock matrix involving up to four center integrals [13]. The numerical free-atom basis sets selected are $2s2p$ atomic orbitals including spin orbitals for carbon atoms.

We gratefully acknowledge the support of the National Natural Science Foundation of China.

*Email address: wlguo@nuaa.edu.cn

[1] W. Lu *et al.*, Science **297**, 983 (2002).
[2] Q. M. Zhang *et al.*, Nature (London) **419**, 284 (2002).
[3] Q. M. Zhang, V. Bharti, and X. Zhao, Science **280**, 2101 (1998).
[4] R. Pelrine, R. Kornbluh, Q. Pei, and J. Joseph, Science **287**, 836 (2000).
[5] E. W. H. Jager, E. Smela, and O. Inganas, Science **290**, 1540 (2000).
[6] M. M. Treacy, T. W. Ebbesen, and J. M. Gibson, Nature (London) **381**, 678 (1996); E. Wong, P. Sheehan, and C. Lieber, Science **277**, 1971 (1997); M. P. Campbell,

C. J. Brabec, and J. Bernholc, Comput. Mater. Sci. **8**, 341 (1997).
[7] R. F. Service, Science **281**, 940 (1998).
[8] R. H. Baughman *et al.*, Science **284**, 1340 (1999).
[9] S. Ghosh, A. K. Sood, and N. Kumar, Science **299**, 1042 (2003).
[10] J. Kong *et al.*, Science **287**, 622 (2000).
[11] M. S. Lavine, Science **298**, 499 (2002).
[12] Z. L. Wang *et al.*, Mater. Sci. Eng. C **16**, 3 (2001).
[13] Y. Guo and W. Guo, J. Phys. D **36**, 805 (2003).
[14] Q. M. Zhang, V. Bharti, and X. Zhao, Science **280**, 2101 (1998).
[15] S. Han and J. Ihm, Phys. Rev. B **61**, 9986 (2000); C. Kim *et al.*, Appl. Phys. Lett. **79**, 1187 (2001).
[16] J-M. Bonard *et al.*, Diam. Relat. Mater. **11**, 763 (2002).